Chapter 1

Introduction

More than 100 years ago, Rutherford's famous scattering experiment discovered the atom was composed of a small but massive nucleus [1]. Rutherford scattered relativistic particles off a fixed target and by measuring the angular products was able to propose the existence of a nucleus. His technique provided the blue prints to study the nucleus over the next century and with higher energies and new probes the nucleus was as well found to have a substructure. The nucleus is now known to be composed of protons and neutrons which are collectively called nucleons.

With still higher energy scattering experiments the nucleons were found to be composite particles as well. In 1964 Gell-Mann and Zweig proposed the quark model to describe the substructure of nucleons [2, 3]. In the quark model the proton is composed of two u-quarks and a d-quark. Quarks were defined as elementary particles with fractional electric charge and a spin of 1/2. Later Feynman proposed the parton model to explain the results of deep inelastic scatter (DIS) experiments [4]. In the parton model, DIS scattering takes place between a distribution of partons inside a nucleon. Later these two theories were unified by the theory of quantum chromodynamics (QCD) which described the nucleon as being held to together by force carrier gluons. In the QCD model, a nucleon is composed of a distribution of valence quarks surrounded by sea quarks and gluons. The valence quarks are responsible for the charge of the nucleon as the sea quarks occur in quark-antiquark pairs. QCD is now the accepted theory for describing the dynamics inside a nucleon.

While there is a theory to describe the quark and gluon interactions, there is currently no theory to describe the bound dynamics of quarks and gluons inside a nucleon. Instead the bound nuclear properties are input as parameters. High energy hadron scattering can be factorized as a hard scattering process multiplied by a soft non-perturbative scattering process. The hard scattering can be calculated ab initio using perturbative QCD, while the soft scattering, on the other hand, is parameterized as the hadron structure or a fragmentation process. Both the hadron structure and fragmentation processes are determined experimentally as either parton distribution functions (PDF) or fragmentation functions (FF) respectively. The former describes how quarks and gluons are bound in a hadron while the latter describes the probability for a quark to fragment into a detectable hadron.

The quark and gluon parton distribution functions have been determined with increasing precision from QCD analysis of DIS, Drell-Yan and semi-inclusive deep inelastic scattering (SIDIS) high energy experiments. When the scattered nucleon has large momentum, the PDFs describe the parton distributions in longitudinal momentum space along the direction of the nucleon's momentum. The most recent theories of the nucleon attempt to give a three dimensional tomographic image of the quark and gluon structure which extend beyond the longitudinal picture to include transverse effects. The extended distributions include either transverse position or transverse momentum to the nucleon's momentum. The former are described by generalized parton distributions (GPD) and the latter are described by transverse momentum dependent (TMD) PDFs. This thesis focuses on TMDs.

A unique way to probe TMDs is by studying transverse spin effects. Polarizing the nucleon transverse to it's momentum gives access to the internal nucleon structure which cannot be accessed from spin averaged experiments. As an example the Sivers TMD PDF is a correlation between transverse spin of the nucleon and transverse momentum of a constituent parton [5]. It therefore makes sense that the only way to measure the Sivers function is through transverse spin experiments.

The first TMDs were proposed to explain the results from large single-spin asymmetries (SSA). A SSA is defined as a normalized difference between spin related counts from a given reaction. One SSA, for example, is the normalized difference between left and right counts from a transversely polarized beam. This left-right asymmetry was first measured in 1976 and found to be non-zero in proton-proton collisions [6]. The Sivers function was proposed to describe large SSAs which lead to a the theoretical frame work of TMDs and is the subject of this thesis.

This thesis is organized into nine chapters. Chapter 2 provides the theoretical and experimental background needed to describe the analysis results in this thesis. Chapter **??** describes the data taking setup, particularly by describing the experimental apparatus and the beam. Chapter **??** gives details on the DC05 detector which was needed for data taking and which the author of this thesis helped construct and maintain. Chapter **??** provides details on the spectrometer alignment which is a crucial preprocessing step for reconstructing data and which the author of this thesis was responsible for in 2015. Chapters **??**- **??** go over the author's analysis techniques, results and conclusions and chapter **??** provides a final summary and conclusion.

Chapter 2

Theoretical and Experimental Overview

2.1 Deep Inelastic Scattering

To understand the structure of the nucleon it is useful to first introduce the original process which described the nucleon as having a sub-structure. This process is the Deep Inelastic Scattering (DIS) process where a lepton impinges on a nucleon denoted as

$$l(\ell) + N(P) \rightarrow l(\ell') + X(P_X), \tag{2.1}$$

where l denotes a lepton, N denotes a nucleon, X represents all products not detected and ℓ, ℓ', P and P_X are the four momentum for their respective lepton or nucleon. This process is an electromagnetic reaction where a lepton is scattered via virtual photon exchange with the nucleon. The leading order Feynman diagram for this reaction is shown in Fig. 2.1.

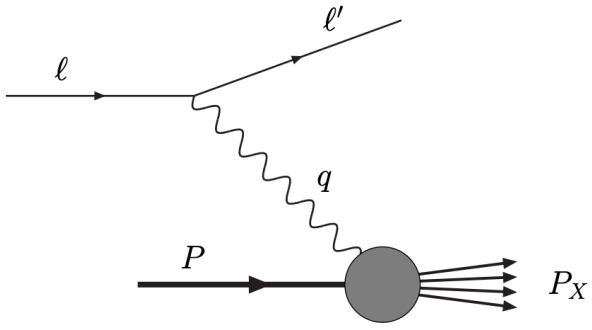

Figure 2.1: The leading order Feynman diagram for deep inelastic scattering

DIS is traditionally studied with a high energy lepton beam and a fixed nuclear target. The initial state kinematics are described by

$$s = (\ell + P)^2 \quad \text{or} \quad E, \tag{2.2}$$

where s is the center of mass energy and E is the energy of the lepton beam. The detected reaction kinematics in the lab frame are described by

$$Q^2 = -q^2 = -(\ell - \ell')^2 \approx EE'(1 - \cos\theta) \qquad (2.3) \qquad x = \frac{Q^2}{2P \cdot q} = \frac{Q^2}{2M\nu} \qquad (2.4)$$

$$\nu = E - E' \qquad (2.5) \qquad y = \frac{P \cdot q}{P \cdot \ell} = \frac{E - E'}{E} = \frac{\nu}{E} \qquad (2.6)$$

$$W^2 = (P + q)^2 \qquad (2.7)$$

where q is the virtual photon four momentum, E' is the scattered lepton's energy, x is Bjorken x, ν is the change in energy of the scattered lepton, y is the inelasticity and W^2 is the invariant mass of the hadron final state. In the last relation from Eq. 2.3, θ is the scattering angle of the lepton with respect to the beam and the approximation is only true when the lepton mass is assumed to be zero. This assumption and the assumption that a quark's mass is zero will be made throughout this thesis. In Eq. 2.4, M is the nucleon mass.

In the parton model, section 2.2, x has the interpretation as being the longitudinal momentum fraction of the struck parton with respect to its parent hadron and therefore x ranges between 0 and 1. The inelasticity, y, measures the proportional energy reduction of the lepton and therefore it's value ranges between 0 and 1.

The process is called deep if $Q^2 >> M^2$ and inelastic if $y < 1$. For practical purposes, in experiments, the deep inelastic criteria corresponds to a $Q^2 > 1\ GeV$ and $W^2 > M^2$. As can be seen in Eq. [2.3-2.7], not all the variables are independent. DIS is described by two independent variables usually given by (x, Q^2) or (x, y). For reference, in the limit as $y \to\ 1$ the process becomes elastic scattering and can then be described by only one independent variable.

The differential cross-section for DIS is defined as [7]

$$\mathrm{d}\sigma = \frac{1}{4P \cdot \ell}\frac{e^4}{Q^4} L_{\mu\nu} W^{\mu\nu} 2\pi \frac{\mathrm{d}^3\ell'}{(2\pi)^3 2E'} \qquad (2.8)$$

where $L_{\mu\nu}$ is the leptonic tensor and $W^{\mu\nu}$ is the hadronic tensor. The leptonic tensor describes free leptons and can therefore be calculated in perturbation theory. It can be decomposed into a systematic spin-independent tensor and an anti-symmetric spin-dependent tensor. Summing over all the possible spins of the lepton beam, the leptonic tensor is

$$L_{\mu\nu} = 2\Big(\ell_\mu \ell'_\nu + \ell_\nu \ell'_\mu - g_{\mu\nu}\ell \cdot \ell'\Big) + 2m\epsilon_{\mu\nu\rho\sigma} s^\rho q^\sigma \qquad (2.9)$$

where m is the lepton mass and s^ρ is the spin four vector of the lepton.

Generically the hadronic tensor is defined as

$$W^{\mu\nu} = \frac{1}{2\pi}\int \mathrm{d}^4\xi e^{iq\cdot\xi}\langle PS|J^\mu(\xi)J^\nu(0)|PS\rangle \tag{2.10}$$

where J is an electromagnetic current and $|PS\rangle$ represents the nucleon with momentum P and spin S. The hadronic tensor describes a hadron bound together by quantum chromo-dynamics (QCD). As of yet there is no known technique for calculating the hadronic tensor in a perturbation theory or otherwise. Instead the hadronic tensor can be written in the most general Lorentz invariant form using structure functions to parameterize the non-perturbative nature of the tensor. With the use of these structure functions, the differential DIS cross-section can be written

$$\frac{\mathrm{d}\sigma}{\mathrm{d}x\mathrm{d}y} = \frac{8\pi\alpha^2 ME}{Q^4}\Big\{xy^2F_1(x,Q^2) + \Big(1-y\Big)\frac{F_2(x,Q^2)}{x} + c_1(y,\frac{Q^2}{\nu})g_1(x,Q^2) + c_2(y,\frac{Q^2}{\nu})g_2(x,Q^2)\Big\} \tag{2.11}$$

where α is the electromagnetic coupling constant; F_1, F_2, g_1, g_2 are structure functions; and c_1 and c_2 are functions which depend on the polarization of the target. The SLAC collaboration measured the structure functions, F_1 and F_2, and found mild variations as a function of Q^2 [8, 9]. This phenomenon now known as Bjorken scaling lead to the theory of the parton model where the DIS reaction no longer depends on Q^2 [10]. Fig. 2.2 shows the F_2 structure function which is approximately constant as a function of Q^2.

2.2 The Parton Model

The parton model is described in an infinite momentum frame which for practical measurements is defined as the frame where the nucleon is moving with momentum larger than it's invariant mass. In the parton model the nucleon, in high energy scattering processes, is considered to be composed of point like constituent massless particles called partons. At high energy scattering the QCD strong force, binding the partons together, becomes asymptotic small and therefore the partons appear to be free. The cross-section in DIS can then be described as a lepton scattering incoherently off a free parton in the nucleon. In the parton model the hadron tensor for scattering off a quark can be written as [7]

$$\begin{aligned} W^{\mu\nu} = \frac{1}{2\pi}\sum_q e_q^2 \sum_X \int \frac{\mathrm{d}^3P_X}{(2\pi)^3 2E_X}\int\frac{\mathrm{d}^4k}{(2\pi)^4}\int\frac{\mathrm{d}^4k'}{(2\pi)^4}\delta(k'^2) \\ \times[\bar{u}(k')\gamma^\mu\langle X|u(k)|PS\rangle]\times[\bar{u}(k')\gamma^\nu\langle X|u(k)|PS\rangle]\times(2\pi)^4\delta^{(4)}(P-k-P_X)(2\pi)^4\delta^{(4)}(k+q-k'), \end{aligned} \tag{2.12}$$

where e_q is the electric charge of quark flavor q and $u(\bar{u})$ is a free Dirac spinor. This hadronic tensor can be

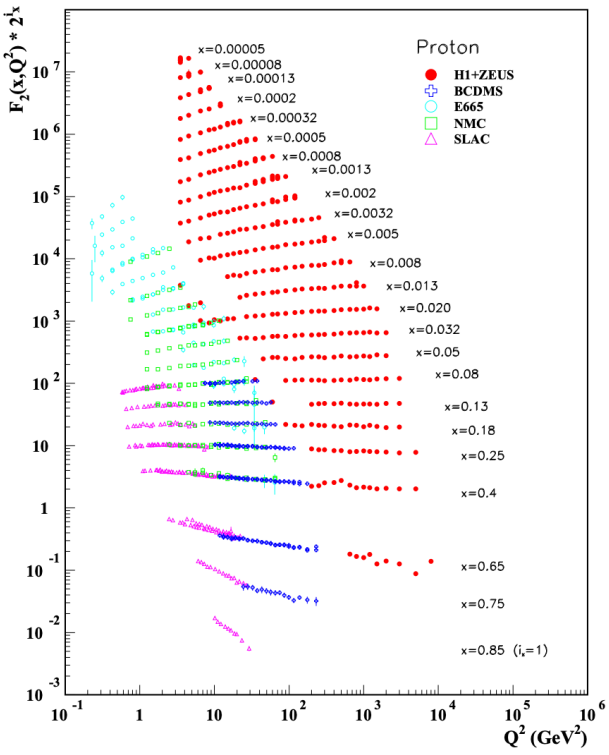

Figure 2.2: The F_2 structure function measured by several experiments. Note that the data is shifted up by a factor 2^{i_x} to see the x dependence. Image taken from [11]

simplified by introducing the quark-quark correlation matrix as

$$\Theta_{ij}(k,P,S) = \sum_X \int \frac{\mathrm{d}^3 P_X}{(2\pi)^3 2E_X}(2\pi)^4\delta^{(4)}(P-k-P_X) \times \langle PS|\phi_j(0)|X\rangle\langle X|\phi_i(0)|PS\rangle, \tag{2.13}$$

where $\phi(\xi) = e^{-ip\cdot\xi}u(p)$ is a quark field. Using the quark-quark correlation matrix, the hadronic tensor can be written as

$$W^{\mu\nu} = \sum_q e_q^2 \int \frac{\mathrm{d}^4 k}{(2\pi)^4} \int \frac{\mathrm{d}^4 k'}{(2\pi)^4}\delta(k'^2)(2\pi)^4\delta^{(4)}(k+q-k') \times \mathrm{Tr}[\Theta\gamma^\mu \not{k}'\gamma^\nu]. \tag{2.14}$$

In the cases of unpolarized or longitudinally polarized DIS the lead order contributing terms from the quark-quark correlator are [12–14]

$$\Theta = \frac{1}{2}\Big(f_1(x)\not{P} + g_{1L}(x)\lambda\gamma_5\not{P}\Big) \tag{2.15}$$

where λ is the longitudinal polarization of the hadron. In this case, the hadronic tensor simplifies to a symmetric contribution and an anti-symmetric contribution as [7]

$$W_{\mu\nu}^{\text{symmetric}} = \frac{1}{P\cdot q}\sum_q e_q^2\Big((k_\mu+q_\mu)P_\nu + (k_\nu+q_\nu)P_\mu - g_{\mu\nu}\Big)f_1^q(x), \tag{2.16}$$

$$W_{\mu\nu}^{\text{anti-symmetric}} = \lambda\epsilon_{\mu\nu\rho\sigma}(k_\nu+q_\nu)P^\rho\sum_q e_q^2 g_{1L}^q(x), \tag{2.17}$$

where in Eq. 2.15-2.17, f_1 and g_1 are parton distribution functions (PDFs).

f_1 is interpreted as the quark number density and g_{1L} is interpreted as the total quark helicity distribution in a hadron. f_1 refers to the density of unpolarized quarks in a hadron and g_{1L} refers to the net density of quarks longitudinally polarized in the same longitudinal direction as the hadron. To make this explicit, f_1 and g_{1L} can be written

$$f_1 = f_1^+ + f_1^-, \tag{2.18}$$

$$g_{1L} = f_1^+ - f_1^-, \tag{2.19}$$

where +(-) denotes the helicity. To be clear while there is a relationship between the two functions, Eq. 2.21, the parton distribution g_{1L} is not the same as the structure function g_1.

The unpolarized quark number density, f_1, has been extracted from global analysis of several experiments [15]. Fig. 2.3 shows the current xf_1 values and confidence intervals for different quarks and gluons in the proton.

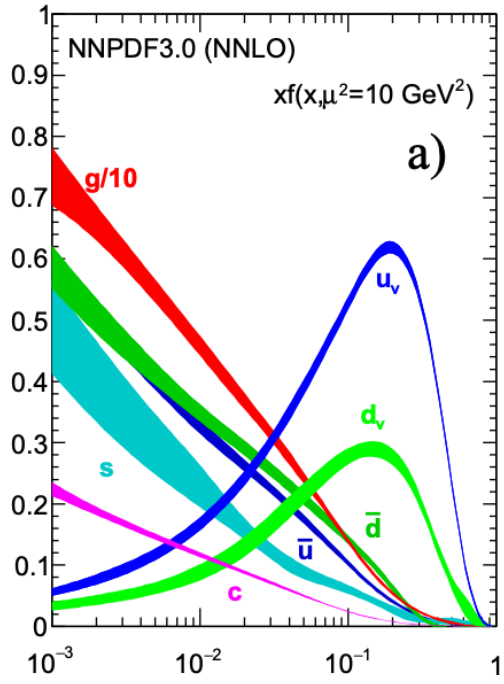

Figure 2.3: The unpolarized parton distribution functions times the momentum fraction. The different colors correspond to different quarks or gluons. Image taken from [11]

The longitudinal spin structure, g_{1L}, has also been measured at SMC, HERMES, and COMPASS [16–18]. The global analysis fit is shown in Fig. 2.4 using the parameterizations from NNPDF2014, AAC2008, DSSV2008 and LSS2010 [19–22].

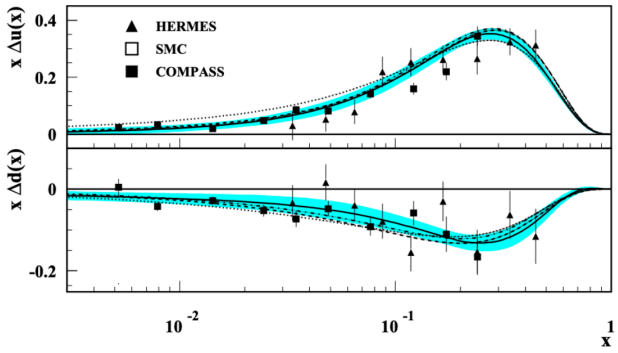

Figure 2.4: The longitudinally polarized parton distribution functions times the momentum fraction for the u-quark (top) and the d-quark (bottom) in a proton. Image taken from [11]

In the parton model the structure function F_1 and F_2 are related to each other and to the unpolarized quark number as

$$F_2(x) = 2xF_1(x) = \sum_q e_q^2 x\Big(f_1^q + f_1^{\bar{q}}\Big) \tag{2.20}$$

which is known as the Callan-Gross relation [23]. As well the structure function g_1 is related to the helicity distribution, g_{1L}, as

$$g_1(x) = \frac{1}{2}\sum_q e_q^2 g_{1L}(x). \tag{2.21}$$

2.3 Transverse Momentum Dependence

In deep inelastic scattering the detected final state lepton is not sensitive to the parton's transverse momentum. That is when measuring the DIS cross-section, all transverse parton momentums are possible which therefore means the scattered parton's transverse momentum is integrated over. As a result, DIS cannot be used to study parton's transverse momentum dependence. The Drell-Yan process 2.5 and the SIDIS process 2.4 however are sensitive to the internal transverse momentum of the partons. In the limit of small transverse momentum compared to the virtual photon momentum, the most generic leading order quark-quark correlator including the transverse parton momentum can be written [12–14]

$$\Theta = \frac{1}{2}\Big[f_1(x,k_\perp)\not{P} + \frac{1}{M}h_1^\perp(x,k_\perp)\sigma^{\mu\nu}k_\mu P_\nu + g_{1L}(x,k_\perp)\lambda\gamma_5\not{P} + \frac{1}{M}g_{1T}(x,k_\perp)\gamma_5\not{P}(k_\perp\cdot S_\perp) + \frac{1}{M}h_{1L}(x,k_\perp)\lambda i\sigma_{\mu\nu}\gamma_5 P^\mu k_\perp^\nu + h_1(x,k_\perp)i\sigma_{\mu\nu}\gamma_5 P^\mu S_\perp^\nu + \frac{1}{M^2}h_{1T}^\perp(x,k_\perp)i\sigma_{\mu\nu}\gamma_5 P^\mu\Big(k_\perp\cdot S_\perp k_\perp^\nu - \frac{1}{2}k_\perp^2 S_\perp^\nu\Big) + \frac{1}{M}f_{1T}^\perp(x,k_\perp)\epsilon^{\mu\nu\rho\sigma}\gamma_\mu P_\nu k_\rho S_\sigma\Big], \tag{2.22}$$

where $k_\perp$ denotes the transverse parton momentum and $S_\perp$ denotes the transverse hadron spin. Eq. 2.22 includes eight transverse momentum dependent (TMD) PDFs which are functions of x and $k_\perp$.

The notation used to depict the TMD functions is the so-called Amsterdam notation. The letters represent the different quark polarizations where f, g, h stand for unpolarized, longitudinally polarized and transversely polarized respectively. The subscript 1 denotes leading order and the subscripts T and L denote a transversely polarized hadron and a longitudinally polarized hadron respectively. Finally the superscript $\perp$ denotes that the distribution is the coefficient of a term where the in which the parton's transverse momentum Lorentz indices are not contracted. Fig. 2.5 organizes the TMDs by nucleon and quark polarizations and gives a visual of each TMD's interpretation.

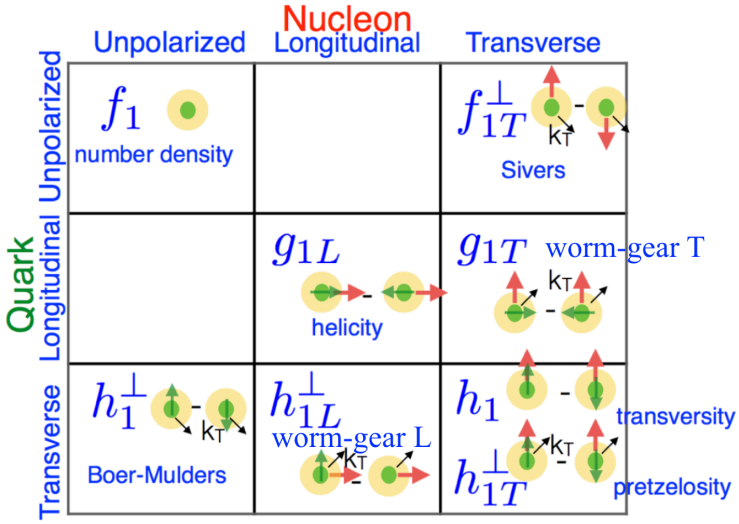

Figure 2.5: The eight TMDs needed to describe a spin 1/2 nucleon at leading order. The columns represent the different nucleon polarizations and the rows represent the different quark polarizations. The individual figures give a visual representation of the TMD's interpretation.

The TMD functions needed to describe Drell-Yan scattering from a transversely polarized target, as in the data taking conditions in this thesis are: the Sivers function, the Boer-Mulders function, the transversity function and the pretzelosity function.

2.3.1 Sivers and Boer-Mulders Distributions

The Sivers TMD, $f_{1,T}^{q\perp}(x, \mathbf{k_T})$, was first purposed to explain large nucleon spin-dependent asymmetries [5]. The interpretation of the Sivers, $f_{1,T}^{q\perp}(x, \mathbf{k_T})$, TMD is that it gives a correlation between transverse spin of the parent hadron and transverse momentum of the scattered parton. When viewing the hadron in the direction opposite to it's momentum and using the sign conventions in this thesis, if $f_{1,T}^{q\perp}(x, \mathbf{k_T})$ is positive then it is expected that there are more partons with momentum pointing left than pointing to the right. A non-zero $f_{1,T}^{q\perp}(x, \mathbf{k_T})$ then implies that the bound partons in a transversely polarized hadron are traveling transverse to the hadron's momentum which can intuitively make senses if the partons have orbital angular momentum. As of yet however, there is no theoretical link between orbital angular momentum and the Sivers function.

The Boer-Mulders TMD PDF, $h_1^\perp$, was proposed in 1998 as a correlation between the transverse momentum and the transverse spin of a parton inside an unpolarized hadron [13]. The Boer-Mulders function is interpreted as a difference between quarks with transverse momentum and transverse spin up and quarks with transverse momentum and transverse spin down in an unpolarized hadron. It is not hard to realized that changing the chirality of transversely polarized quarks in an unpolarized hadron would flip the sign of the Boer-Mulders function which therefore means the Boer-Mulders function is chiral odd. Chiral odd functions can only be non-zero when convoluted with another chiral odd function as is the case when the Boer-Mulders function appears in either the SIDIS or Drell-Yan cross-section.

The most surprising fact about the Sivers and Boer-Mulders functions is that they both changes sign under naive time reversal. Naive time reversal is defined as reversing time but not swapping initial and final states [14]. The Sivers and Boer-Mulders functions are therefore said to be T-odd functions, and as a result, were originally believe to be forbidden correlations. However it was shown that the Sivers function could be non-zero from gluon exchange during the initial state in the Drell-Yan process and gluon exchange during the final state in the SIDIS process [24, 25]. Most surprisingly, it was shown that a non-zero Sivers function and a non-zero Boer-Mulders function are expected to have opposite sign in SIDIS and Drell-Yan [26]. That is

$$f_{1T}^\perp|_{Drell-Yan} = -f_{1T}^\perp|_{SIDIS}, \tag{2.23}$$

$$h_1^\perp|_{Drell-Yan} = -h_1^\perp|_{SIDIS}. \tag{2.24}$$

2.3.2 Transversity and Pretzelosity

Unlike the Sivers and Boer-Mulders TMDs, the transversity, $h_1(x, k_T)$, and pretzelosity, $h_{1T}^{\perp}$, TMDs are predicted to be universal functions of a spin 1/2 hadron. The transversity is defined for transversely polarized hadrons as the difference between quarks polarized in the same direction as their parent hadron and quarks polarized in the opposite direction to their parent hadron. The transversity distribution is then similar to the helicity distribution, g_{1L}, but for transverse polarizations. The pretzelosity function is a correlation between transversely polarized partons and their transverse momentum in a transversely polarized hadron. As with the Boer-Mulders TMD, both the transversity and the pretzelosity TMDs are chiral odd and are therefore convoluted with another chiral odd function.

2.4 Semi-Inclusive Deep Inelastic Scattering

Semi-Inclusive Deep Inelastic Scattering (SIDIS) is the process where a lepton scatters electromagnetically off a nucleon and subsequently the scattered lepton and at least one scattered hadron are detected. As the name implies, SIDIS is related to the DIS reaction only SIDIS includes the addition of a detected hadron. SIDIS is denoted as

$$l(\ell, \lambda_l) + N(P, S) \rightarrow l(\ell') + h(P_h) + X(P_X), \tag{2.25}$$

where λ_l is the helicity of the incoming lepton, S is the spin of the nucleon, h is the detected hadron and P_h is the detected hadron's four momentum. The leading order one photon exchange Feynman diagram for the SIDIS process is shown in Fig. 2.6.

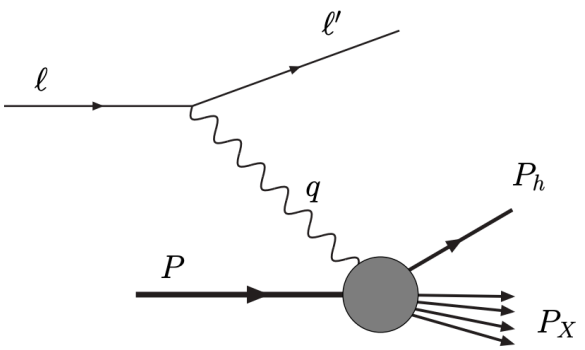

Figure 2.6: The semi-inclusive deep inelastic scattering leading order Feynman diagram

In addition to the kinematic variables used to describe DIS, Eq. [2.3-2.7], one more variable is needed to

describe the SIDIS process,

$$z = \frac{P \cdot P_h}{P \cdot q} \overset{lab}{\underset{frame}{=}} \frac{E_h}{E - E'}, \tag{2.26}$$

which is interpreted as the fraction of possible energy the detected hadron can obtain. The transverse spin-dependent SIDIS cross-section can be described in a model independent way using structure functions as [14]

$$\begin{aligned}
\frac{d\sigma}{dx\, dy\, d\psi\, dz\, d\phi_h\, dP_{h\perp}^2} = \frac{\alpha^2}{xyQ^2} \frac{y^2}{2\,(1-\varepsilon)} \left(1 + \frac{\gamma^2}{2x}\right) \Bigg\{ & F_{UU,T} + \varepsilon F_{UU,L} + \sqrt{2\,\varepsilon(1+\varepsilon)}\, \cos\phi_h\, F_{UU}^{\cos\phi_h} \\
& + \varepsilon \cos(2\phi_h)\, F_{UU}^{\cos 2\phi_h} + \lambda_l \sqrt{2\,\varepsilon(1-\varepsilon)}\, \sin\phi_h\, F_{LU}^{\sin\phi_h} \\
& + |S_\perp| \Bigg[\sin(\phi_h - \phi_S) \left(F_{UT,T}^{\sin(\phi_h - \phi_S)} + \varepsilon\, F_{UT,L}^{\sin(\phi_h - \phi_S)} \right) \\
& \qquad + \varepsilon\, \sin(\phi_h + \phi_S)\, F_{UT}^{\sin(\phi_h + \phi_S)} + \varepsilon\, \sin(3\phi_h - \phi_S)\, F_{UT}^{\sin(3\phi_h - \phi_S)} \\
& \qquad + \sqrt{2\,\varepsilon(1+\varepsilon)}\, \sin\phi_S\, F_{UT}^{\sin\phi_S} + \sqrt{2\,\varepsilon(1+\varepsilon)}\, \sin(2\phi_h - \phi_S)\, F_{UT}^{\sin(2\phi_h - \phi_S)} \Bigg] \\
& + |S_\perp| \lambda_l \Bigg[\sqrt{1-\varepsilon^2}\, \cos(\phi_h - \phi_S)\, F_{LT}^{\cos(\phi_h - \phi_S)} + \sqrt{2\,\varepsilon(1-\varepsilon)}\, \cos\phi_S\, F_{LT}^{\cos\phi_S} \\
& \qquad + \sqrt{2\,\varepsilon(1-\varepsilon)}\, \cos(2\phi_h - \phi_S)\, F_{LT}^{\cos(2\phi_h - \phi_S)} \Bigg] \Bigg\},
\end{aligned} \tag{2.27}$$

where

$$\varepsilon = \frac{1 - y - \frac{1}{4}\gamma^2 y^2}{1 - y + \frac{1}{2}y^2 + \frac{1}{4}\gamma^2 y^2}, \tag{2.28}$$

and $\gamma = \frac{2Mx}{Q}$, ψ is the azimuthal scattering angle of the lepton around the lepton beam with respect to the transverse spin direction of the target and where this cross-section is defined in the γ-nucleon reference frame. The γ-nucleon reference system is a lab frame where the virtual photon is along the z-axis and the xz-plane is determined by the lepton plane. Fig. 2.7 shows the γ-nucleon lab frame and the relevant azimuthal angles.

The 14 structure functions in Eq. 2.27 are coefficients to the azimuthal angles from the γ-nucleon reference frame. The structure functions are label as F where the superscript denotes which azimuthal angle coefficient they correspond to and the three subscripts represent the beam, target and virtual photon polarization from left to right respectively. The subscript polarizations are U for unpolarized, L for longitudinally polarized and T for transversely polarized. The cross-section, Eq. 2.27, is determined similarly to the DIS cross-section,

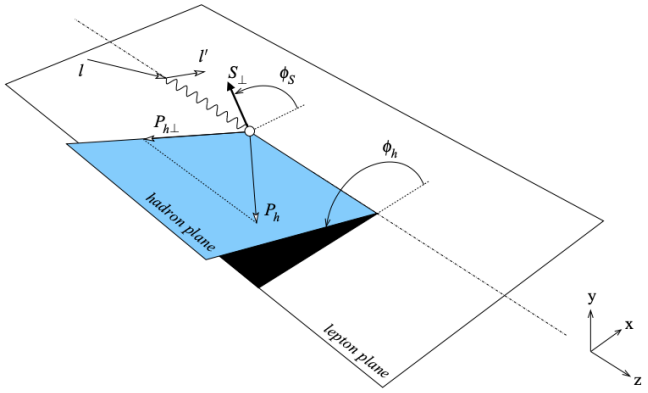

Figure 2.7: The γ-nucleon lab frame where the target nucleon is at rest and the virtual photon is along the z-axis. The lepton scattering plane defines the xz-plane where the outgoing lepton defines the positive x-direction. This image was taken from [14].

Eq. 2.11, in that structure functions are used to generically parameterize the hadronic tensor.

In the TMD regime the structure functions are related to TMD functions and fragmentation functions (FF). For SIDIS, the TMD regime is defined as the detected hadron's transverse momentum being small compared to the virtual photon momentum, $P_{hT} << Q$. Then in this regime the model independent structure functions are equal to a convolution of a TMD and a FF where the convolution is defined as

$$\mathcal{C}[w(p_T, k_T) f D] = x \sum_q e_q^2 \int d^2 p_T d^2 k_T \delta^{(2)}(p_T - k_T - P_{h\perp}/z) w(p_T, k_T) f^q(x, p_T^2) D^q(z, k_T^2), \tag{2.29}$$

where w is a weight f is a TMD function and D is a FF. For the structure functions related to transverse target polarization, the relations between structure functions and TMDs at leading order are [14]

$$F_{UT,T}^{\sin(\phi_h-\phi_S)} = \mathcal{C}\left[-\frac{\hat{h}\cdot p_T}{M} f_{1T}^{\perp} D_1\right] \qquad \propto f_{1T}^{\perp}\otimes D_1, \tag{2.30}$$

$$F_{UT,L}^{\sin(\phi_h-\phi_S)} = 0, \tag{2.31}$$

$$F_{UT}^{\sin(\phi_h+\phi_S)} = \mathcal{C}\left[-\frac{\hat{h}\cdot k_T}{M_h} h_1 H_1^{\perp}\right] \qquad \propto h_1\otimes H_1^{\perp}, \tag{2.32}$$

$$F_{UT}^{\sin(3\phi_h-\phi_S)} = \mathcal{C}\left[\frac{2(\hat{h}\cdot p_T)(\boldsymbol{p}_T\cdot k_T)+\boldsymbol{p}_T^2(\hat{h}\cdot k_T)-4(\hat{h}\cdot p_T)^2(\hat{h}\cdot k_T)}{2M^2M_h} h_{1T}^{\perp} H_1^{\perp}\right] \qquad \propto h_{1T}^{\perp}\otimes H_1^{\perp}, \tag{2.33}$$

$$F_{LT}^{\cos(\phi_h-\phi_S)} = \mathcal{C}\left[\frac{\hat{h}\cdot p_T}{M} g_{1T} D_1\right] \qquad \propto g_{1T}\otimes D_1, \tag{2.34}$$

and the leading order structure functions related to an unpolarized target are

$$F_{UU,T} = \mathcal{C}[f_1 D_1] \qquad \propto f_1\otimes D_1, \tag{2.35}$$

$$F_{UU,L} = 0 \tag{2.36}$$

$$F_{UU}^{\cos 2\phi_h} = \mathcal{C}\left[-\frac{2(\hat{h}\cdot k_T)(\hat{h}\cdot p_T)-k_T\cdot p_T}{MM_h} h_1^{\perp} H_1^{\perp}\right] \qquad \propto h_1^{\perp}\otimes H_1^{\perp}, \tag{2.37}$$

where the unit vector $\hat{h} = P_{h\perp}/|P_{h\perp}|$ and D_1 and $H_1^{\perp}$ are fragmentation functions.

The fragmentation functions are functions of z and describe the probability for a quark to hadronize to a specific hadron. These fragmentation functions depend on the quark spin, the hadron type and polarization, and the quark k_T. In Eq. [2.30- 2.36] the fragmentation function D_1 refers to an unpolarized quark fragmenting to an unpolarized hadron and $H_1^{\perp}$ refers to a transversely polarized quark fragmenting to an unpolarized hadron.

The SIDIS cross-section, Eq. 2.27, can be rewritten in terms of asymmetries. These asymmetries are defined as

$$A_{BeamTarget}^{w_i(\phi_h,\phi_S)} = \frac{F_{BeamTarget}^{w_i(\phi_h,\phi_S)}}{F_{UU,T}+\varepsilon F_{UU,L}}, \tag{2.38}$$

where $w_i(\phi_h,\phi_S)$ is the azimuthal angle associated with this asymmetry and $Beam$ and $Target$ represent the polarization of the beam and target. The asymmetry amplitude, Eq. 2.38, is a structure function divide by the unpolarized structure functions. This asymmetry amplitude definition is defined because it is easier to measure experimentally. In order to determine an asymmetry amplitudes, the number of counts experimentally measured are fit using a function in the form of Eq. 2.27. The parameters of this fit are

the coefficients to each azimuthal amplitude. The results of the fit can then determine the spin-dependent asymmetry amplitudes without needing to determine luminosity and therefore have reduced systematic errors.

2.4.1 SIDIS TMD Results

COMPASS and HERMES measuremented the asymmetry $A_{UT,T}^{\sin(\phi_h-\phi_S)}$ from the SIDIS reaction from a transversely polarized proton target [27, 28]. The comparison of the results between these two collaborations is shown in Fig. 2.8. The asymmetry amplitude $A_{UT,T}^{\sin(\phi_h-\phi_S)}$ is related to the Sivers function and was measured to be non-zero at a level up to 5%.

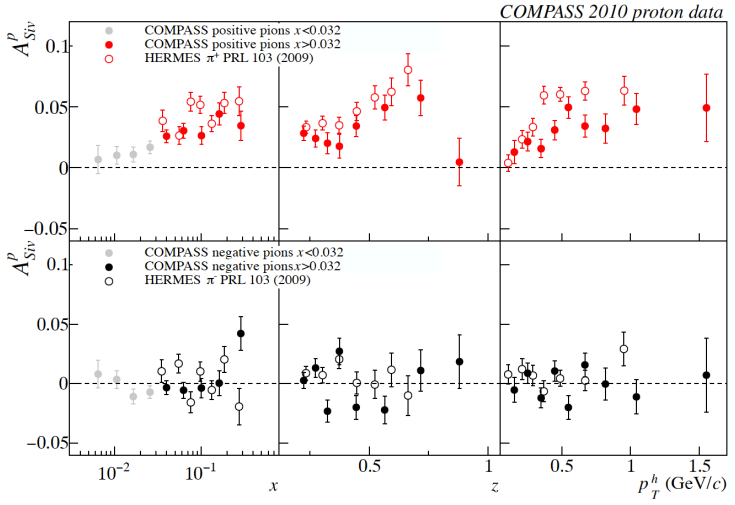

Figure 2.8: The asymmetry amplitude related to the Sivers function measure by COMPASS [27] and HERMES [28]

The top plot in Fig. 2.8 is the asymmetry for a positive detected hadron. A positively detected final state hadron is dominated by u-quark scattering and therefore by the u-quark Sivers function. This is the case for three reasons. Firstly because the SIDIS reaction is weighted by e_q^2 which therefore makes the u-quark scattering four times more likely. Secondly the so-called favored FF, where the detected hadron is the same charge as the quark which fragmented, is larger than the unfavored FF. Therefore a positively detected hadron most likely resulted from a positively fragmenting quark. Thirdly the proton target is composed of twice as many u-quarks as d-quarks in this scattering kinematic region. For these three reasons the results in Fig. 2.8 imply that the u-quark Sivers function from the SIDIS reaction is positive.

The bottom plots in Fig. 2.8 suggest that the d-quark Sivers function in the SIDIS reaction is negative. The bottom results in Fig. 2.8 are from the combination of u-quark scattering and fragmenting unfavoredly and d-quark scattering and fragmenting favoredly. As was mentioned the charge weighting in the SIDIS

reaction and the proton quark composition results in the u-quark scattering with a higher probability. On the other hand the previous effect is canceled out by the fact that the favor FF for the d-quark fragmenting is larger than the unfavored FF for the u-quark fragmenting. Therefore the results in the bottom of Fig. 2.8 are for an approximately equal combination from u-quark scattering and d-quark scattering. As the u-quark asymmetry amplitude is positive, the d-quark asymmetry amplitude must therefore be negative and so also must the d-quark Sivers function. Anselmino et. al. extracted the Sivers function using both HERMES and COMPASS data and additional data for fragmentation functions [29]. These results are shown in Fig. 2.9.

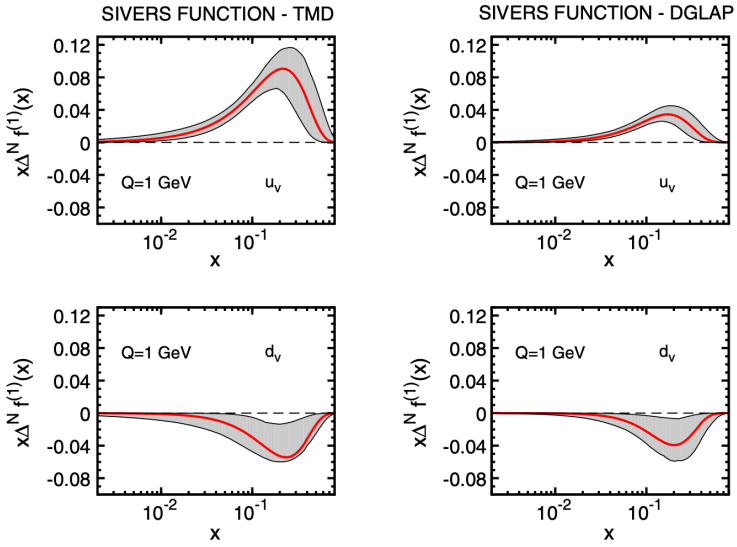

Figure 2.9: The valence quark distributions for the first moment of the Sivers function. The left plots are using TMD evolution and the right plots are using DGLAP evolution to globally include all measured data. This image was taken from [29]

Results for the TMD asymmetry amplitude, $A_{UU}^{\cos 2\phi_h}$, related to the Boer-Mulders function were measured by the COMPASS collaboration from SIDIS [30]. As can be seen from the convolution of the structure function, Eq. 2.37, and the definition of asymmetry amplitudes in SIDIS, Eq. 2.38, this asymmetry amplitude is a convolution of the Boer-Mulders function and a fragmentation function. The COMPASS results for $A_{UU}^{\cos 2\phi_h}$ are shown in Fig. 2.10. Notably the Boer-Mulders asymmetry amplitude is higher for negatively scattered hadrons than for positively scattered hadrons suggesting that the Boer-Mulders function is larger for d-quarks than for u-quarks.

Three SIDIS experiments measured data related to the transversity distribution from the structure function $F_{UT}^{\sin(\phi_h+\phi_S)}$. These three experiments were HERMES [31, 32], COMPASS [27, 33–36], and JLab HALL A [37]. The FF data to determine $H_1^\perp$ from the structure function, $F_{UT}^{\sin(\phi_h+\phi_S)}$, comes from BELLE [38, 39] and BABAR [40] data in e^+e^- annihilation data. Anselmino et. al. extracted the transversity distribution [41] from all this data and their results are shown in Fig. 2.11.

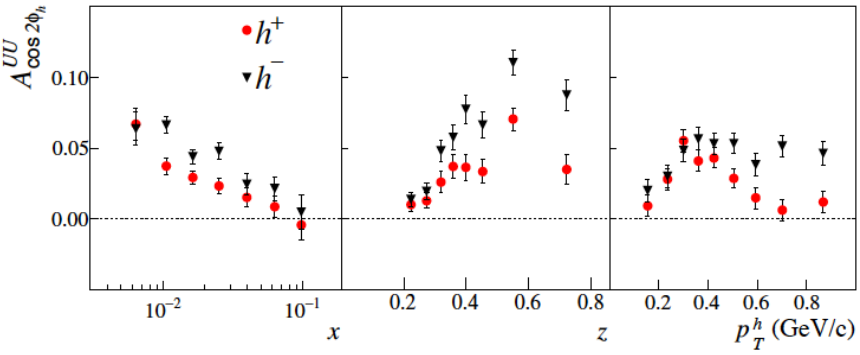

Figure 2.10: COMPASS SIDIS data from muons scattered off of a deuteron target for positively scatted hadrons (red) and negatively scattered hadrons (black). The asymmetry amplitude is related to the Boer-Mulders functions. This image was taken from [30]

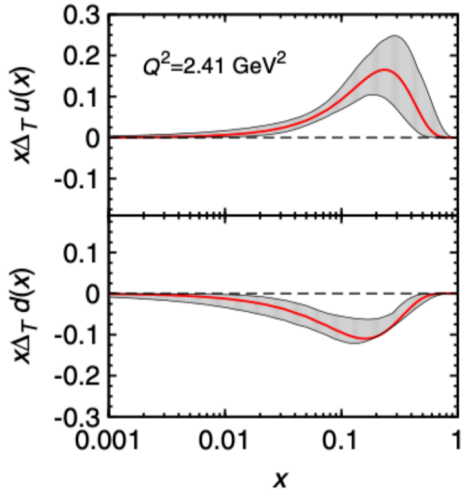

Figure 2.11: The transversity distribution for u-quarks (top) and d-quarks (bottom) determined from SIDIS data and e^+e^- data. Image taken from [41].

2.5 Drell-Yan

The Drell-Yan process is the reaction where a quark and an anti-quark annihilate and the end product results in two detected leptons. The Drell-Yan process is denoted as

$$H_a(P_a) + H_b(P_b, S) \rightarrow \gamma^* + X \rightarrow l(\ell) + l'(\ell') + X \tag{2.39}$$

where H_a and H_b are hadrons which carry the quark and anti-quarks and in this thesis only the target hadron, H_b is considered to be polarized with spin S. In this thesis the quark and anti-quark pair annihilate to form a virtual photon, γ^* and additionally the only final state detected leptons considered are a muon

and an anti-muon pair. The leading order one photon exchange diagram is shown in Fig. 2.12.

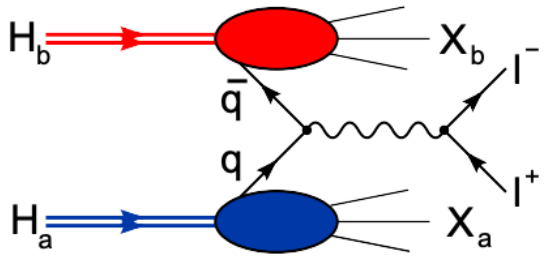

Figure 2.12: The Drell-Yan leading order diagram

The angles used to define the general Drell-Yan cross-section are defined with the use of two reference frames. The target frame (TF), Fig. 2.13a, defines the ϕ_S angle and the Collins-Soper (CS), Fig. 2.13b, frame defines the additional ϕ and θ angles. The ϕ_S angle is defined in the TF as the angle between the transverse momentum of the virtual photon and the transverse spin of the target. The ϕ and θ angles, in the CS frame, are defined as the azimuthal and polar angle of the negatively charged muon.

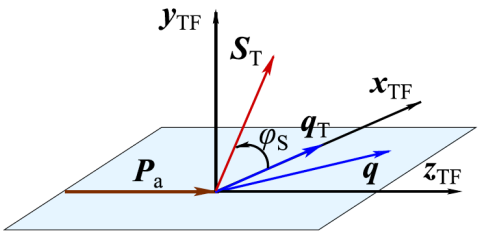

(a) The target frame where the z-axis is along the beam and the x-axis is in the direction of the transverse momentum of the virtual photon.

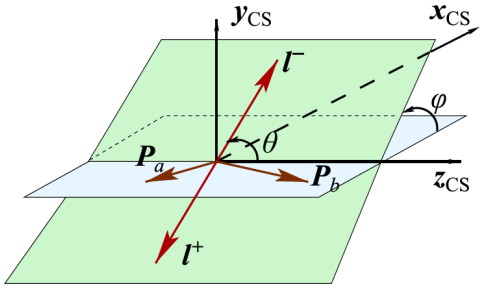

(b) The Collins-Soper frame is defined in the rest frame of the virtual photon where the z-axis bisects the beam and target momentum vectors.

The target frame is defined in the lab frame where the beam is along the z-axis and the transverse momentum of the virtual photon is along the x-axis. The y-axis in the target frame is then chosen so the coordinate system is right handed. The Collins-Soper frame is defined in the rest frame of the virtual photon where the xz-plane coincides with the hadron plane and the z-axis is chosen so it bisects the momentum vectors P_a and $-P_b$. The CS frame is defined from the target frame as a boost first along the along z-axis and then a boost along the x-axis so the rest frame of the virtual photon is reached.

The leading order model independent Drell-Yan differential cross-section for a polarized target is [42, 43]

$$\frac{d\sigma}{d^4q\,d\Omega} = \frac{\alpha_{em}^2}{F\,q^2}\Big\{\Big((1+\cos^2\theta)\,F_U^1 + (1-\cos^2\theta)\,F_U^2 + \sin 2\theta\cos\phi\,F_U^{\cos\phi} + \sin^2\theta\cos 2\phi\,F_U^{\cos 2\phi}\Big)$$
$$+ S_L\Big(\sin 2\theta\sin\phi\,F_L^{\sin\phi} + \sin^2\theta\sin 2\phi\,F_L^{\sin 2\phi}\Big)$$
$$+ |S_T|\Big[\Big(F_T^{\sin\phi_S} + \cos^2\theta\,\tilde{F}_T^{\sin\phi_S}\Big)\sin\phi_S + \Big(F_T^{\sin(\phi+\phi_S)}\,\sin(\phi+\phi_S) + F_T^{(\sin\phi-\phi_S)}\,\sin(\phi-\phi_S)\Big)\sin 2\theta$$
$$+ \Big(F_T^{\sin(2\phi+\phi_S)}\,\sin(2\phi+\phi_S) + F_T^{\sin(2\phi-\phi_S)}\,\sin(2\phi-\phi_S)\Big)\sin^2\theta\Big]\Big\}, \tag{2.40}$$

where $F = 4\sqrt{(P_a\cdot P_b)^2 - M_a^2M_b^2}$ is the flux and Ω is the solid angle of the outgoing negatively charged muon. The twelve model independent structure functions in Eq. 2.40 are labeled as $F_{Target\ polarization}^{azimuthal\ angle\ coefficient}$. The phase space when the TMD regime is valid in DY scattering is when $q_T << q$. In this regime the structure functions are equal to a convolution of a beam and a target TMD function where convolution is defined similarly to the SIDIS case, Eq. 2.29, as

$$\mathcal{C}[w(k_{aT},k_{bT})f_a\bar{f}_b] = \frac{1}{N_c}\sum_q e_q^2\int d^2k_{aT}d^2k_{bT}\delta^{(2)}(q_T - k_{aT} - k_{bT})$$
$$\times\, w(k_{aT},k_{bT})\Big[f_a^q(x,k_{aT}^2)f_b^{\bar{q}}(x,k_{bT}^2) + f_a^{\bar{q}}(x,k_{aT}^2)f_b^q(x,k_{bT}^2)\Big], \tag{2.41}$$

where $N_c = 3$ is the number of color charges. The leading order DY structure functions in the TMD phase space are related to TMD functions as [42]

$$F_U^1 = \mathcal{C}[f_1 \bar{f}_1] \qquad \propto f_{1,Beam}^{\bar{u}} \otimes f_{1,Target}^{u}, \tag{2.42}$$

$$F_U^{\cos 2\phi} = \mathcal{C}\left[\frac{2(\vec{h}\cdot\vec{k}_{aT})(\vec{h}\cdot\vec{k}_{bT}) - \vec{k}_{aT}\cdot\vec{k}_{bT}}{M_a M_b} h_1^{\perp}\bar{h}_1^{\perp}\right] \qquad \propto h_{1,Beam}^{\perp\,\bar{u}} \otimes h_{1,Target}^{\perp\,u}, \tag{2.43}$$

$$F_L^{\sin 2\phi} = -\mathcal{C}\left[\frac{2(\vec{h}\cdot\vec{k}_{aT})(\vec{h}\cdot\vec{k}_{bT}) - \vec{k}_{aT}\cdot\vec{k}_{bT}}{M_a M_b} h_1^{\perp}\bar{h}_{1L}^{\perp}\right] \qquad \propto h_{1,Beam}^{\perp\,\bar{u}} \otimes h_{1L,Target}^{\perp\,u}, \tag{2.44}$$

$$F_T^1 = -\mathcal{C}\left[\frac{\vec{h}\cdot\vec{k}_{bT}}{M_b} f_1 \bar{f}_{1T}^{\perp}\right] \qquad \propto f_{1,Beam}^{\bar{u}} \otimes f_{1T,Target}^{\perp\,u}, \tag{2.45}$$

$$F_T^{\sin(2\phi-\phi_S)} = -\mathcal{C}\left[\frac{\vec{h}\cdot\vec{k}_{aT}}{M_a} h_1^{\perp}\bar{h}_1\right] \qquad \propto h_{1,Beam}^{\perp\,\bar{u}} \otimes h_{1,Target}^{u}, \tag{2.46}$$

$$F_T^{\sin(2\phi+\phi_S)} = -\mathcal{C}\left[\frac{2(\vec{h}\cdot\vec{k}_{bT})[2(\vec{h}\cdot\vec{k}_{aT})(\vec{h}\cdot\vec{k}_{bT}) - \vec{k}_{aT}\cdot\vec{k}_{bT}] - \vec{k}_{bT}^2(\vec{h}\cdot\vec{k}_{aT})}{2M_a M_b^2} h_1^{\perp}\bar{h}_{1T}^{\perp}\right] \qquad \propto h_{1,Beam}^{\perp\,\bar{u}} \otimes h_{1T,Target}^{\perp\,u}, \tag{2.47}$$

where $\vec{h} = \vec{q}_T/q_T$ is a unit vector and furthermore the assumption in this thesis is that the beam $\bar{u}$-quark annihilates with the target u-quark. The additional leading order structure functions are zero

$$F_U^2 \;=\; F_U^{\cos\phi} \;=\; F_L^{\sin\phi} \;=\; F_T^2 \;=\; F_T^{\sin(\phi-\phi_S)} \;=\; F_T^{\sin(\phi+\phi_S)} \;= 0. \tag{2.48}$$

The differential cross-seciton, Eq. 2.40, can be rewritten in terms of asymmetry amplitudes and depolarization factors. The asymmetry amplitudes are defined similarly to the case in SIDIS, Eq. 2.38, and again for the reason that asymmetries can be determined to a higher precision than structure functions. For Drell-Yan these asymmetry amplitudes are

$$A_{Target}^{w_i(\phi,\phi_S)} = \frac{F_{Target}^{w_i(\phi,\phi_S)}}{F_U^1 + F_U^2}. \tag{2.49}$$

The asymmetry amplitudes are the result of different virtual photon polarizations decaying to a final state lepton pair. The depolarization factor is defined as the ratio of the virtual photon polarization to produce

such an asymmetry to that of a transversely polarized virtual photon. The depolarization is defined for each asymmetry amplitude as

$$D_{[f(\theta)]} = \frac{f(\theta)}{1 + A_U^1 \cos^2\theta}, \tag{2.50}$$

where the function $f(\theta)$ corresponds to virtual photon angular decay responsible for the given asymmetry. The Drell-Yan differential cross-section, Eq. 2.40, now simplifies to [43]

$$\begin{aligned}\frac{d\sigma}{d^4q\, d\Omega} = \frac{\alpha_{em}^2}{F\, q^2}\hat{\sigma}_U \Big\{ &\Big(1 + D_{[\sin^2\theta]} \cos 2\phi\, A_U^{\cos 2\phi}\Big) \\ &+ S_L D_{[\sin^2\theta]} \sin 2\phi\, A_L^{\sin 2\phi} \\ &+ |S_T| \Big[A_T^{\sin\phi_S} \sin\phi_S + \Big(A_T^{\sin(2\phi+\phi_S)} \sin(2\phi+\phi_S) + A_T^{\sin(2\phi-\phi_S)} \sin(2\phi-\phi_S)\Big) D_{[\sin^2\theta]} \Big] \Big\}, \end{aligned} \tag{2.51}$$

where $\hat{\sigma}_U = F_U^1(1+\cos^2\theta)$ is the unpolarized DY cross-section. For the data taking conditions in 2015 it is assumed that the target is transversely polarized so $S_L = 0$ and therefore the Drell-Yan cross-section can be simplified to

$$\begin{aligned}\frac{d\sigma}{d^4q\, d\Omega} = \frac{\alpha_{em}^2}{F\, q^2}\hat{\sigma}_U \Big\{ &\Big(1 + D_{[\sin^2\theta]} \cos 2\phi\, A_U^{\cos 2\phi}\Big) \\ &+ |S_T| \Big[A_T^{\sin\phi_S} \sin\phi_S + \Big(A_T^{\sin(2\phi+\phi_S)} \sin(2\phi+\phi_S) + A_T^{\sin(2\phi-\phi_S)} \sin(2\phi-\phi_S)\Big) D_{[\sin^2\theta]} \Big] \Big\}. \end{aligned} \tag{2.52}$$

2.5.1 Drell-Yan Sivers Result

The first Drell-Yan results for the Sivers asymmetry amplitude, in an attempt to verify the sign change between Drell-Yan and SIDIS, came from hadron-hadron collisions at Star [44]. Their result measured the Sivers amplitude from $pp^\uparrow \to Z^0 X$ and $pp^\uparrow \to W^\pm X$ and are shown in Fig. 2.14. The statistical error bars are too high and the Q^2 scale is very different from that used to measure a Sivers function in SIDIS however. As of the data of this thesis it is impossible to conclude on a sign change of the Sivers function between Drell-Yan and SIDIS.

2.5.2 Left-Right Asymmetry

An asymmetry of interest for measuring high energy spin related phenomena is the analyzing power. This asymmetry is denoted A_N and is responsible for a left-right asymmetry for a suitable definition of left and

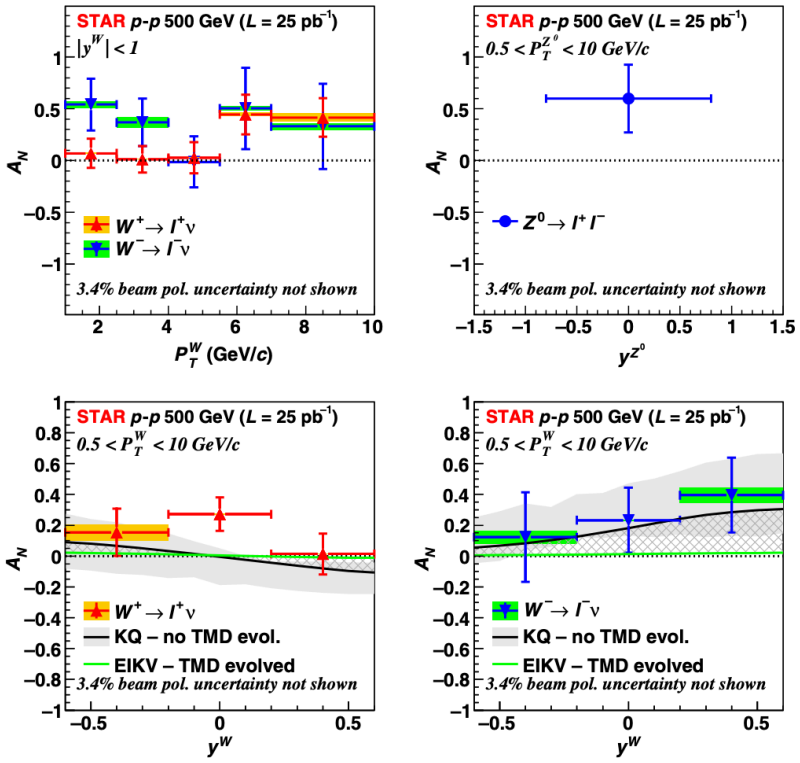

Figure 2.14: All plots show a left-right asymmetry which is related to the Sivers function. The top right plot is for Z^0 production while the other three plots are for $W^{\pm}$ production. Q^2 evolution and resulting error bars from EIKV [45] and KQ [46]. Image taken from [44].

right. The cross-section for spin 1/2 particles scattering where one of the initial particles is polarized can be written

$$I(\theta, \phi) = I_0(\theta)(1 + SA_N \cos(\phi)) \tag{2.53}$$

where I_0 is the unpolarized cross-section, S is the beam or target polarization percentage and ϕ is the azimuthal scattering angle of the outgoing measured particle. Working in the target frame for Drell-Yan scattering from a transversely polarized target, the azimuthal angle can be redefined in terms of the ϕ_S angle by noting that $\phi = \frac{\pi}{2} - \phi_S$. Eq. 2.53 can then be written in the form of the Drell-Yan cross-section, Eq. 2.51, as

$$\begin{aligned}\frac{d\sigma}{d^4q\,d\phi_S} &= \frac{\alpha_{em}^2}{F\,q^2}\hat{\sigma}_U\Big(1+|S_T|A_N\cos(\frac{\pi}{2}-\phi_S)\Big) \\ &= \frac{\alpha_{em}^2}{F\,q^2}\hat{\sigma}_U\Big(1+|S_T|A_N\sin(\phi_S)\Big) \\ &= \frac{\alpha_{em}^2}{F\,q^2}\hat{\sigma}_U\Big(1+|S_T|A_T^{\sin\phi_S}\sin(\phi_S)\Big),\end{aligned} \tag{2.54}$$

where this relation is obtained from Eq. 2.51 by integrating over all angle except ϕ_S and where the polarization S is assumed to be transverse. Therefore the analyzing power, A_N, is the same as the Sivers asymmetry amplitude, $A_T^{\sin\phi_S}$, for Drell-Yan scattering.

An analysis technique for measuring A_N is by making a left-right asymmetry. The left-right asymmetry is defined as

$$A_{lr} = \frac{1}{|S_T|}\frac{\sigma_l-\sigma_r}{\sigma_l+\sigma_r}, \tag{2.55}$$

where $\sigma_{l(r)}$ is the cross-section for producing a final state to the left(right). In the target frame the definition of left scattering is $\int_{\phi_S=0}^{\phi_S=\pi}\frac{d\sigma}{d^4q\,d\phi_S}d\phi_S$ and definition of right scattering is $\int_{\phi_S=\pi}^{\phi_S=2\pi}\frac{d\sigma}{d^4q\,d\phi_S}d\phi_S$. It is straight forward to show the relationship between A_{lr} and A_N as

$$\begin{aligned}A_{lr} &= \frac{1}{|S_T|}\frac{\int_{\phi_S=0}^{\phi_S=\pi}\frac{d\sigma}{d^4q\,d\phi_S}d\phi_S - \int_{\phi_S=\pi}^{\phi_S=2\pi}\frac{d\sigma}{d^4q\,d\phi_S}d\phi_S}{\int_{\phi_S=0}^{\phi_S=\pi}\frac{d\sigma}{d^4q\,d\phi_S}d\phi_S + \int_{\phi_S=\pi}^{\phi_S=2\pi}\frac{d\sigma}{d^4q\,d\phi_S}d\phi_S} \\ &= \frac{1}{|S_T|}\frac{\phi_S-|S_T|A_N\cos\phi_S\Big|_0^{\pi} - \Big(\phi_S-|S_T|A_N\cos\phi_S\Big)\Big|_{\pi}^{2\pi}}{\phi_S-|S_T|A_N\cos\phi_S\Big|_0^{\pi} + \Big(\phi_S-|S_T|A_N\cos\phi_S\Big)\Big|_{\pi}^{2\pi}} \\ &= \frac{1}{|S_T|}\frac{4|S_T|A_N}{2\pi} \\ &= \frac{2A_N}{\pi}.\end{aligned} \tag{2.56}$$

Another method to determine A_N, is with the transverse spin asymmetry (TSA) defined as

$$\begin{aligned}A_{TSA} =& \frac{1}{|S_T|}\frac{\frac{d\sigma^{\uparrow}}{d\phi_s}-\frac{d\sigma^{\downarrow}}{d\phi_s}}{\frac{d\sigma^{\uparrow}}{d\phi_s}+\frac{d\sigma^{\downarrow}}{d\phi_s}} \\ =& \frac{1}{|S_T|}\frac{1+|S_T|A_N\sin\phi_S-\Big(1+|S_T|A_N\sin(\phi_S+\pi)\Big)}{1+|S_T|A_N\sin\phi_S+\Big(1+|S_T|A_N\sin(\phi_S+\pi)\Big)} \\ =& A_N\sin\phi_S.\end{aligned} \tag{2.57}$$

To understand how A_N is related to the Sivers function, it is illustrative to write the Drell-Yan differential cross-section under the TMD assumptions as [46]

$$\frac{d\sigma^{H_a H_b \to l^+ l^- X}}{d\eta dM^2 d^2 q_T} = \hat{\sigma}_0 \sum_q e_q^2 \int d^2 k_{aT} d^2 k_{bT} \delta^{(2)}(k_{aT} + k_{bT} - q_T) f_{\bar{q}/H_a}(x_a, k_{aT}) f_{q/H_b}(x_b, k_{bT}), \tag{2.58}$$

η is rapidity and $f_{\bar{q}(q)/H_{a(b)}}$ is a TMD function. Inserting this cross-section into the transverse spin asymmetry, Eq. 2.57, and using proper TMD functions for the given transverse polarization gives

$$\begin{aligned} A_{TSA} &= A_N \sin\phi_S \\ &= -\frac{1}{S} \frac{\sum_q e_q^2 \int d^2 k_{aT} d^2 k_{bT} \delta^{(2)}(k_{aT} + k_{bT} - q_T) f_{\bar{q}/H_a}(x_a, k_{aT}) \frac{k_{bT}}{M_b} f_{1T}^{\perp q}(x_b, k_{bT}) S \sin\phi_S}{\sum_q e_q^2 \int d^2 k_{aT} d^2 k_{bT} \delta^{(2)}(k_{aT} + k_{bT} - q_T) f_{\bar{q}/H_a}(x_a, k_{aT}) f_{q/H_b}(x_b, k_{bT})}. \end{aligned} \tag{2.59}$$

Several experiments measured large values for A_N at different center of mass energies. Fig. 2.15 shows the results of A_N from hadron-hadron collisions from four different experiments over a range of center of mass energies.

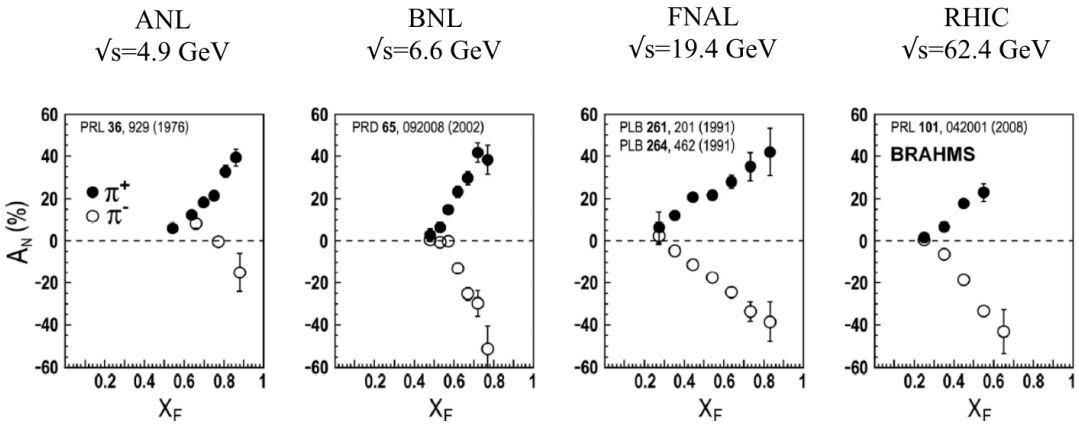

Figure 2.15: Large A_N values where found at ANL [6], BNL [47], FNAL [48, 49] and RHIC [50].

2.5.3 Weighted Asymmetries from Drell-Yan

The proton TMD functions, determined from Drell-Yan in Eqs. 2.42-2.47, are convoluted with a TMD function from the beam pion. The Drell-Yan convolution, Eq. 2.41, makes it difficult to determine a single TMD function and for this reason model assumptions are made in the global analysis to extract the individual TMDs from the convolutions. An alternative method involving weighted asymmetries however, makes it possible to disentangle the convolution and determine a k_T^2 moment of a TMD function both for SIDIS [13, 51, 52] and for Drell-Yan [53–56].

The deconvolution by weighted asymmetries works by multiplying a given structure function by an appropriate weight and integrating over the virtual photon transverse momentum, q_T. The simplest Drell-Yan structure function to deconvolute is F_U^1. By integrating Eq. 2.42 over q_T the convolution equation becomes

$$\begin{aligned}
\int d^2q_T F_U^1 &= \int d^2q_T \mathcal{C}[f_{1,a}\bar{f}_{1,b}] \\
&= \int d^2q_T \frac{1}{N_c}\sum_q e_q^2 \int d^2k_{aT} d^2k_{bT} \delta^{(2)}(q_T - k_{aT} - k_{bT}) \\
&\qquad \times \Big[f_{1,a}^q(x_a, k_{aT}^2) f_{1,b}^{\bar{q}}(x_b, k_{bT}^2) + f_{1,a}^{\bar{q}}(x_a, k_{aT}^2) f_{1,b}^q(x_b, k_{bT}^2) \Big] \\
&= \frac{1}{N_c}\sum_q e_q^2 f_{1,a}^q(x_a) f_{1,b}^{\bar{q}}(x_b) + f_{1,a}^{\bar{q}}(x_a) f_{1,b}^q(x_b) \\
&\overset{COMPASS}{\approx} \frac{4}{27} f_{1,\pi}^{\bar{u}}(x_\pi) f_{1,proton}^u(x_{proton}),
\end{aligned} \tag{2.60}$$

where $f_1(x) = \int d^2k_T f_1(x, k_T^2)$ is a TMD function integrated over k_T. In Eq. 2.60 the weight was 1 and no assumptions were needed to perform the integration. The answer is a TMD function for the beam multiplied by a TMD function from the target. The final equality in Eq. 2.60 is valid in the COMPASS kinematic region and shows how straight forward this method can make TMD extraction.

Deconvoluting the additional Drell-Yan structure functions, Eqs 2.43-2.47, is similar to Eq. 2.60 but requires a different weight. The Sivers TMD function can be extracted from the F_T^1 structure function using a weight equal to $|q_T|/M_b$. This can be seen by multiplying F_T^1 by the weight $|q_T|/M_b$, and integrating over q_T to remove the Dirac delta function as follows

$$\begin{aligned}
\int d^2q_T \frac{|q_T|}{M_b} F_T^1 &= -\int d^2q_T \frac{|q_T|}{M_b} \mathcal{C}\Big[\frac{\vec{q}_T \cdot \vec{k}_{bT}}{|q_T| M_b} f_{1,a}\bar{f}_{1T,b}^{\perp}\Big] \\
&= -\int d^2q_T \frac{|q_T|}{M_b}\frac{1}{N_c}\sum_q e_q^2 \int d^2k_{aT} d^2k_{bT} \delta^{(2)}(q_T - k_{aT} - k_{bT}) \\
&\qquad \times \frac{\vec{q}_T \cdot \vec{k}_{bT}}{|q_T| M_b} \Big[f_{1,a}^q(x_a, k_{aT}^2) f_{1T,b}^{\bar{q}\perp}(x_b, k_{bT}^2) + f_{1,a}^{\bar{q}}(x_a, k_{aT}^2) f_{1T,b}^{q\perp}(x_b, k_{bT}^2) \Big] \\
&= -\frac{1}{N_c}\sum_q e_q^2 \int d^2k_{aT} d^2k_{bT} \times \frac{(\vec{k}_{aT} + \vec{k}_{bT}) \cdot \vec{k}_{bT}}{M_b^2} \Big[f_{1,a}^q(x_a, k_{aT}^2) f_{1T,b}^{\bar{q}\perp}(x_b, k_{bT}^2) + f_{1,a}^{\bar{q}}(x_a, k_{aT}^2) f_{1T,b}^{q\perp}(x_b, k_{bT}^2) \Big].
\end{aligned} \tag{2.61}$$

To simplify further we make use of the fact that the unpolarized quark distribution function is even in k_T

which means

$$\int_{-\infty}^{\infty} d^2k_{aT}\vec{k}_{aT}\cdot\vec{k}_{bT}f_{1,a}(x_a,k_{aT}^2)=0, \tag{2.62}$$

and therefore only even terms in k_T^2 need to be considered. Eq. 2.61 can then be further simplified as

$$\begin{aligned}\int d^2q_T\frac{|q_T|}{M_b}F_T^1 &= -\frac{2}{N_c}\sum_q e_q^2\Big[f_{1,a}^q(x_a)f_{1T,b}^{(1)\bar{q}\perp}(x_b)+f_{1,a}^{\bar{q}}(x_a)f_{1T,b}^{(1)q\perp}(x_b)\Big] \\ &\overset{COMPASS}{\approx} -\frac{8}{27}f_{1,\pi}^{\bar{u}}(x_\pi)f_{1T,proton}^{(1)u\perp}(x_{proton}),\end{aligned} \tag{2.63}$$

where the $f_{1T}^{(1)q\perp}(x)=\int d^2k_T\frac{k_T^2}{2M}f_{1T}^{q\perp}(x,k_T^2)$ is the first k_T^2 moment of the Sivers function and the general k_T moment of a TMD is defined as $f^{(n)}(x)=\int d^2k_T\Big(\frac{k_T^2}{2M}\Big)^n f(x,k_T^2)$.

The essential steps in deconvolution the TMD functions are to multiply by a weight which gets rid of any q_T terms outside of the Dirac delta function and to only include even terms in k_T. The remaining two transverse spin-dependent structure functions can also be deconvoluted in a similar fashion to give

$$\begin{aligned}\int d^2q_T\frac{|q_T|^3}{2M_aM_b^2}F_T^{\sin(2\phi+\phi_S)} &= -\frac{2}{N_c}\sum_q e_q^2\Big[h_{1,a}^{(1)\bar{q}\perp}(x_a)h_{1T,b}^{(2)q\perp}(x_b)+(q\leftrightarrow\bar{q})\Big] \\ &\overset{COMPASS}{\approx} -\frac{8}{27}h_{1,\pi}^{(1)\bar{u}\perp}(x_\pi)\;h_{1T,proton}^{(2)u\perp}(x_{proton}),\end{aligned} \tag{2.64}$$

$$\begin{aligned}\int d^2q_T\frac{|q_T|}{M_a}F_T^{\sin(2\phi-\phi_S)} &= -\frac{2}{N_c}\sum_q e_q^2\Big[h_{1,a}^{(1)\bar{q}\perp}(x_a)h_{1,b}^{(2)q}(x_b)+(q\leftrightarrow\bar{q})\Big] \\ &\overset{COMPASS}{\approx} -\frac{8}{27}h_{1,\pi}^{(1)\bar{u}\perp}(x_\pi)\;h_{1,proton}^{(2)u}(x_{proton}),\end{aligned} \tag{2.65}$$

where Eq. 2.64 can be used to determined the proton pretzelosity function and Eq. 2.65 can be used to determine the proton transversity function.

For experimentally determining the k_T^2 moments of TMD functions the following weighted asymmetries amplitudes are defined

$$A^{YW_Y}X(x_a,x_b)=\frac{\int d^2q_T W_Y F_X^Y}{\int d^2q_T F_U^1}, \tag{2.66}$$

where Y is the azimuthal modulation of interest, W_Y is the appropriate weight and X denotes the targets polarization. For example the Sivers weighted asymmetry amplitude is as follows

$$A^{\sin\phi_S \frac{q_T}{M_b}} = \frac{\int d^2q_T \frac{q_T}{M_b} F_T^{\sin\phi_S}}{\int d^2q_T F_U^1} \quad \underset{\approx}{COMPASS} \quad -2\frac{f_{1T,proton}^{(1)u\perp}(x_{proton})}{f_{1,proton}}. \tag{2.67}$$

2.5.4 J/Ψ Production

The production of J/Ψ hadrons potentially offers an alternative mechanism for studying TMD related effects. As of yet however, there is no confirmation on the J/Ψ production mechanism and therefore it impossible to say if TMD effects are present from J/Ψ production. Still there are many models which can be tested, some of which assume TMD functions contribute to produce J/Ψ hadrons.

One of the most popular J/Ψ production models, is the color evaporation model [57]. In this model the J/Ψ production results from gluon-gluon fusion and quark and ant-quark annihilation. This is depicted as

$$\sigma\Big|_{H_a H_b \to J/\Psi X \to l^+ l^- X} = \sigma_{q\bar{q}\to c\bar{c}} + \sigma_{gg\to c\bar{c}}, \tag{2.68}$$

where $\sigma_{q\bar{q}(gg)\to c\bar{c}}$ is the cross-section for quark-quark annihilation (gluon-gluon fusion) to a $c\bar{c}$ final state. In the case of quark-quark annihilation there is interest in a model duality between Drell-Yan and J/Ψ production.

The spin and parity J/Ψ quantum numbers are the same as the spin and parity of a photon. For this reason it is hypothesized that there is a duality between the Drell-Yan process and J/Ψ production [58–60]. This duality transforms the electromagnetic coupling and Drell-Yan invariant mass to a new J/Ψ coupling and J/Ψ mass given as

$$\begin{aligned} \text{Drell}-\text{Yan Production} \quad & \quad \text{J/}\Psi \text{ Production} \\ 16\pi^2\alpha^2 e_q^2 \quad & \to \quad (g_q^{J/\Psi})^2 (g_l^{J/\Psi})^2 \qquad (2.69) \\ \frac{1}{M^4} \quad & \to \quad \frac{1}{(M^2 - M_{J/\Psi}^2)^2 + M_{J/\Psi}^2 \Gamma_{J/\Psi}^2}, \qquad (2.70) \end{aligned}$$

where $M^2 = Q^2$, $M_{J/\Psi}^2 \approx 9.59\ (\text{GeV}/c^2)^2$ is the J/Ψ mass squared and $\Gamma_{J/\Psi}$ is the full J/Ψ width.

This duality is only expected when quark-quark annihilation dominates over gluon-gluon fusion however. Under this duality assumption, the TSA related to the analyzing power offers an interesting avenue for studying TMDs. Assuming quark-antiquark annihilation dominates and that duality relations, Eq 2.69 and Eq. 2.70, are valid then the TSA can be written for J/Ψ production as written [61]

$$A_{TSA}^{J\Psi} = -\frac{1}{S}\frac{\sum_q (g_q^V)^2 \int d^2k_{aT} d^2k_{bT} \delta^{(2)}(k_{aT} + k_{bT} - q_T) f_{\bar{q}/H_a}(x_a, k_{aT}) \frac{k_{bT}}{M_b} f_{1T}^{\perp q}(x_b, k_{bT}) S \sin\phi_S}{\sum_q (g_q^V)^2 \int d^2k_{aT} d^2k_{bT} \delta^{(2)}(k_{aT} + k_{bT} - q_T) f_{\bar{q}/H_a}(x_a, k_{aT}) f_{q/H_b}(x_b, k_{bT})}. \quad (2.71)$$

In the case of COMPASS with $u\bar{u}$ annihilation dominating, then the unknown couplings, g_q^V, cancel and are not needed to study TMD functions.

References

[1] E. Rutherford. The scattering of alpha and beta particles by matter and the structure of the atom. *Phil. Mag. Ser.6*, 21:669–688, 1911. doi: 10.1080/14786440508637080.

[2] Murray Gell-Mann. A Schematic Model of Baryons and Mesons. *Phys. Lett.*, 8:214–215, 1964. doi: 10.1016/S0031-9163(64)92001-3.

[3] G. Zweig. An SU(3) model for strong interaction symmetry and its breaking. Version 2. In D.B. Lichtenberg and Simon Peter Rosen, editors, *DEVELOPMENTS IN THE QUARK THEORY OF HADRONS. VOL. 1. 1964 - 1978*, pages 22–101. 1964.

[4] Richard P. Feynman. Very high-energy collisions of hadrons. *Phys. Rev. Lett.*, 23:1415–1417, Dec 1969. doi: 10.1103/PhysRevLett.23.1415. URL `https://link.aps.org/doi/10.1103/PhysRevLett.23.1415`.

[5] Dennis W. Sivers. Single Spin Production Asymmetries from the Hard Scattering of Point-Like Constituents. *Phys. Rev.*, D41:83, 1990. doi: 10.1103/PhysRevD.41.83.

[6] R. D. Klem, J. E. Bowers, H. W. Courant, H. Kagan, M. L. Marshak, E. A. Peterson, K. Ruddick, W. H. Dragoset, and J. B. Roberts. Measurement of asymmetries of inclusive pion production in proton-proton interactions at 6 and 11.8 gev/c. *Phys. Rev. Lett.*, 36:929–931, Apr 1976. doi: 10.1103/PhysRevLett.36.929. URL `https://link.aps.org/doi/10.1103/PhysRevLett.36.929`.

[7] Vincenzo Barone, Alessandro Drago, and Philip G. Ratcliffe. Transverse polarisation of quarks in hadrons. *Phys. Rept.*, 359:1–168, 2002. doi: 10.1016/S0370-1573(01)00051-5.

[8] Elliott D. Bloom et al. High-Energy Inelastic e p Scattering at 6-Degrees and 10-Degrees. *Phys. Rev. Lett.*, 23:930–934, 1969. doi: 10.1103/PhysRevLett.23.930.

[9] Martin Breidenbach, Jerome I. Friedman, Henry W. Kendall, Elliott D. Bloom, D. H. Coward, H. C. DeStaebler, J. Drees, Luke W. Mo, and Richard E. Taylor. Observed Behavior of Highly Inelastic electron-Proton Scattering. *Phys. Rev. Lett.*, 23:935–939, 1969. doi: 10.1103/PhysRevLett.23.935.

[10] J. D. Bjorken and Emmanuel A. Paschos. Inelastic Electron Proton and gamma Proton Scattering, and the Structure of the Nucleon. *Phys. Rev.*, 185:1975–1982, 1969. doi: 10.1103/PhysRev.185.1975.

[11] M. Tanabashi et al. Review of Particle Physics. *Phys. Rev.*, D98(3):030001, 2018. doi: 10.1103/PhysRevD.98.030001.

[12] P. J. Mulders and R. D. Tangerman. The Complete tree level result up to order 1/Q for polarized deep inelastic leptoproduction. *Nucl. Phys.*, B461:197–237, 1996. doi: 10.1016/S0550-3213(96)00648-7,10.1016/0550-3213(95)00632-X. [Erratum: Nucl. Phys.B484,538(1997)].

[13] Daniel Boer and P. J. Mulders. Time reversal odd distribution functions in leptoproduction. *Phys. Rev.*, D57:5780–5786, 1998. doi: 10.1103/PhysRevD.57.5780.

[14] Alessandro Bacchetta, Markus Diehl, Klaus Goeke, Andreas Metz, Piet J. Mulders, and Marc Schlegel. Semi-inclusive deep inelastic scattering at small transverse momentum. *JHEP*, 02:093, 2007. doi: 10.1088/1126-6708/2007/02/093.

[15] Juan Rojo et. al. The PDF4lhc report on PDFs and LHC data: results from run i and preparation for run II. *Journal of Physics G: Nuclear and Particle Physics*, 42(10):103103, sep 2015. doi: 10.1088/0954-3899/42/10/103103. URL https://doi.org/10.1088%2F0954-3899%2F42%2F10%2F103103.

[16] B. Adeva et al. The Spin dependent structure function g(1) (x) of the proton from polarized deep inelastic muon scattering. *Phys. Lett.*, B412:414–424, 1997. doi: 10.1016/S0370-2693(97)01106-4.

[17] A. et al. Airapetian. Flavor decomposition of the sea-quark helicity distributions in the nucleon from semiinclusive deep inelastic scattering. *Phys. Rev. Lett.*, 92:012005, Jan 2004. doi: 10.1103/PhysRevLett.92.012005. URL https://link.aps.org/doi/10.1103/PhysRevLett.92.012005.

[18] I. A. Savin. COMPASS results on the nucleon spin structure. *Nucl. Phys. Proc. Suppl.*, 219-220:94–101, 2011. doi: 10.1016/j.nuclphysbps.2011.11.001.

[19] L. A. Harland-Lang, A. D. Martin, P. Motylinski, and R. S. Thorne. The impact of the final HERA combined data on PDFs obtained from a global fit. *Eur. Phys. J.*, C76(4):186, 2016. doi: 10.1140/epjc/s10052-016-4020-1.

[20] I. Abt, A. M. Cooper-Sarkar, B. Foster, V. Myronenko, K. Wichmann, and M. Wing. Study of HERA ep data at low Q^2 and low x_{Bj} and the need for higher-twist corrections to standard perturbative QCD fits. *Phys. Rev.*, D94(3):034032, 2016. doi: 10.1103/PhysRevD.94.034032.

[21] Emanuele R. Nocera, Richard D. Ball, Stefano Forte, Giovanni Ridolfi, and Juan Rojo. A first unbiased global determination of polarized PDFs and their uncertainties. *Nucl. Phys.*, B887:276–308, 2014. doi: 10.1016/j.nuclphysb.2014.08.008.

[22] M. Hirai and S. Kumano. Determination of gluon polarization from deep inelastic scattering and collider data. *Nucl. Phys.*, B813:106–122, 2009. doi: 10.1016/j.nuclphysb.2008.12.026.

[23] C. G. Callan and David J. Gross. High-energy electroproduction and the constitution of the electric current. *Phys. Rev. Lett.*, 22:156–159, Jan 1969. doi: 10.1103/PhysRevLett.22.156. URL https://link.aps.org/doi/10.1103/PhysRevLett.22.156.

[24] Stanley J. Brodsky, Dae Sung Hwang, and Ivan Schmidt. Final state interactions and single spin asymmetries in semiinclusive deep inelastic scattering. *Phys. Lett.*, B530:99–107, 2002. doi: 10.1016/S0370-2693(02)01320-5.

[25] Stanley J. Brodsky, Dae Sung Hwang, and Ivan Schmidt. Initial state interactions and single spin asymmetries in Drell-Yan processes. *Nucl. Phys.*, B642:344–356, 2002. doi: 10.1016/S0550-3213(02)00617-X.

[26] John C. Collins. Leading twist single transverse-spin asymmetries: Drell-Yan and deep inelastic scattering. *Phys. Lett.*, B536:43–48, 2002. doi: 10.1016/S0370-2693(02)01819-1.

[27] M. Alekseev et al. Collins and Sivers asymmetries for pions and kaons in muon-deuteron DIS. *Phys. Lett.*, B673:127–135, 2009. doi: 10.1016/j.physletb.2009.01.060.

[28] A. Airapetian et al. Observation of the Naive-T-odd Sivers Effect in Deep-Inelastic Scattering. *Phys. Rev. Lett.*, 103:152002, 2009. doi: 10.1103/PhysRevLett.103.152002.

[29] M. Anselmino, M. Boglione, and S. Melis. Strategy towards the extraction of the sivers function with transverse momentum dependent evolution. *Phys. Rev. D*, 86:014028, Jul 2012. doi: 10.1103/PhysRevD.86.014028. URL https://link.aps.org/doi/10.1103/PhysRevD.86.014028.

[30] C. Adolph et al. Measurement of azimuthal hadron asymmetries in semi-inclusive deep inelastic scattering off unpolarised nucleons. *Nucl. Phys.*, B886:1046–1077, 2014. doi: 10.1016/j.nuclphysb.2014.07.019.

[31] A. Airapetian et al. Single-spin asymmetries in semi-inclusive deep-inelastic scattering on a transversely polarized hydrogen target. *Phys. Rev. Lett.*, 94:012002, 2005. doi: 10.1103/PhysRevLett.94.012002.

[32] A. Airapetian et al. Effects of transversity in deep-inelastic scattering by polarized protons. *Phys. Lett.*, B693:11–16, 2010. doi: 10.1016/j.physletb.2010.08.012.

[33] E. S. Ageev et al. A New measurement of the Collins and Sivers asymmetries on a transversely polarised deuteron target. *Nucl. Phys.*, B765:31–70, 2007. doi: 10.1016/j.nuclphysb.2006.10.027.

[34] M. G. Alekseev et al. Measurement of the Collins and Sivers asymmetries on transversely polarised protons. *Phys. Lett.*, B692:240–246, 2010. doi: 10.1016/j.physletb.2010.08.001.

[35] C. Adolph et al. Experimental investigation of transverse spin asymmetries in muon-p SIDIS processes: Collins asymmetries. *Phys. Lett.*, B717:376–382, 2012. doi: 10.1016/j.physletb.2012.09.055.

[36] C. Adolph et al. Collins and Sivers asymmetries in muonproduction of pions and kaons off transversely polarised protons. *Phys. Lett.*, B744:250–259, 2015. doi: 10.1016/j.physletb.2015.03.056.

[37] X. et. al. Qian. Single spin asymmetries in charged pion production from semi-inclusive deep inelastic scattering on a transversely polarized ^{3}He target at $Q^2 = 1.4 - -2.7$ gev^2. *Phys. Rev. Lett.*, 107: 072003, Aug 2011. doi: 10.1103/PhysRevLett.107.072003. URL `https://link.aps.org/doi/10.1103/PhysRevLett.107.072003`.

[38] Kazuo Abe et al. Measurement of azimuthal asymmetries in inclusive production of hadron pairs in e+ e- annihilation at Belle. *Phys. Rev. Lett.*, 96:232002, 2006. doi: 10.1103/PhysRevLett.96.232002.

[39] R. Seidl et al. Measurement of Azimuthal Asymmetries in Inclusive Production of Hadron Pairs in e+e- Annihilation at s**(1/2) = 10.58-GeV. *Phys. Rev.*, D78:032011, 2008. doi: 10.1103/PhysRevD.78.032011,10.1103/PhysRevD.86.039905. [Erratum: Phys. Rev.D86,039905(2012)].

[40] J. P. Lees et al. Measurement of Collins asymmetries in inclusive production of charged pion pairs in e^+e^- annihilation at BABAR. *Phys. Rev.*, D90(5):052003, 2014. doi: 10.1103/PhysRevD.90.052003.

[41] M. Anselmino, M. Boglione, U. D'Alesio, S. Melis, F. Murgia, and A. Prokudin. Simultaneous extraction of transversity and collins functions from new semi-inclusive deep inelastic scattering and e^+e^- data. *Phys. Rev. D*, 87:094019, May 2013. doi: 10.1103/PhysRevD.87.094019. URL `https://link.aps.org/doi/10.1103/PhysRevD.87.094019`.

[42] S. Arnold, A. Metz, and M. Schlegel. Dilepton production from polarized hadron hadron collisions. *Phys. Rev.*, D79:034005, 2009. doi: 10.1103/PhysRevD.79.034005.

[43] A. Kotzinian. Description of polarized π^- + N Drell-Yan processes, 2010. URL `http://wwwcompass.cern.ch/compass/notes_public/2010-2.pdf`.

[44] L. et. al. Adamczyk. Measurement of the transverse single-spin asymmetry in $p^\uparrow + p \to W^\pm/Z^0$ at rhic. *Phys. Rev. Lett.*, 116:132301, Apr 2016. doi: 10.1103/PhysRevLett.116.132301. URL `https://link.aps.org/doi/10.1103/PhysRevLett.116.132301`.

[45] Miguel G. Echevarria, Ahmad Idilbi, Zhong-Bo Kang, and Ivan Vitev. Qcd evolution of the sivers asymmetry. *Phys. Rev. D*, 89:074013, Apr 2014. doi: 10.1103/PhysRevD.89.074013. URL `https://link.aps.org/doi/10.1103/PhysRevD.89.074013`.

[46] Zhong-Bo Kang and Jian-Wei Qiu. Testing the time-reversal modified universality of the sivers function. *Phys. Rev. Lett.*, 103:172001, Oct 2009. doi: 10.1103/PhysRevLett.103.172001. URL `https://link.aps.org/doi/10.1103/PhysRevLett.103.172001`.

[47] Allgower et. al. Measurement of analyzing powers of π^+ and π^- produced on a hydrogen and a carbon target with a $22 - \mathrm{GeV}/c$ incident polarized proton beam. *Phys. Rev. D*, 65:092008, May 2002. doi: 10.1103/PhysRevD.65.092008. URL `https://link.aps.org/doi/10.1103/PhysRevD.65.092008`.

[48] D.L. Adams et. al. Comparison of spin asymmetries and cross sections in 0 production by 200 gev polarized antiprotons and protons. *Physics Letters B*, 261(1):201 – 206, 1991. ISSN 0370-2693. doi: https://doi.org/10.1016/0370-2693(91)91351-U. URL http://www.sciencedirect.com/science/article/pii/037026939191351U.

[49] D.L. Adams et. al. Analyzing power in inclusive + and production at high xf with a 200 gev polarized proton beam. *Physics Letters B*, 264(3):462 – 466, 1991. ISSN 0370-2693. doi: https://doi.org/10.1016/0370-2693(91)90378-4. URL http://www.sciencedirect.com/science/article/pii/0370269391903784.

[50] Arsene et. al. Single-transverse-spin asymmetries of identified charged hadrons in polarized pp collisions at $\sqrt{s} = 62.4$ GeV. *Phys. Rev. Lett.*, 101:042001, Jul 2008. doi: 10.1103/PhysRevLett.101.042001. URL https://link.aps.org/doi/10.1103/PhysRevLett.101.042001.

[51] A. M. Kotzinian and P. J. Mulders. Longitudinal quark polarization in transversely polarized nucleons. *Phys. Rev.*, D54:1229–1232, 1996. doi: 10.1103/PhysRevD.54.1229.

[52] A. M. Kotzinian and P. J. Mulders. Probing transverse quark polarization via azimuthal asymmetries in leptoproduction. *Phys. Lett.*, B406:373–380, 1997. doi: 10.1016/S0370-2693(97)00708-9.

[53] A. V. Efremov, K. Goeke, S. Menzel, A. Metz, and P. Schweitzer. Sivers effect in semi-inclusive DIS and in the Drell-Yan process. *Phys. Lett.*, B612:233–244, 2005. doi: 10.1016/j.physletb.2005.03.010.

[54] A. N. Sissakian, O. Yu. Shevchenko, A. P. Nagaytsev, and O. N. Ivanov. Direct extraction of transversity and its accompanying T-odd distribution from the unpolarized and single-polarized Drell-Yan process. *Phys. Rev.*, D72:054027, 2005. doi: 10.1103/PhysRevD.72.054027.

[55] A. Sissakian, O. Shevchenko, A. Nagaytsev, O. Denisov, and O. Ivanov. Transversity and its accompanying T-odd distribution from Drell-Yan processes with pion-proton collisions. *Eur. Phys. J.*, C46:147–150, 2006. doi: 10.1140/epjc/s2006-02490-1.

[56] Zhengxian Wang, Xiaoyu Wang, and Zhun Lu. Boer-Mulders function of pion meson and q_T-weighted $\cos 2\phi$ asymmetry in the unpolarized $\pi^- p$ Drell-Yan at COMPASS. *Phys. Rev.*, D95(9):094004, 2017. doi: 10.1103/PhysRevD.95.094004.

[57] R. Vogt. J/ production and suppression. *Physics Reports*, 310(4):197 – 260, 1999. ISSN 0370-1573. doi: https://doi.org/10.1016/S0370-1573(98)00074-X. URL http://www.sciencedirect.com/science/article/pii/S037015739800074X.

[58] M. Anselmino, V. Barone, A. Drago, and N. N. Nikolaev. Accessing transversity via J / psi production in polarized p vector anti-p vector interactions. *Phys. Lett.*, B594:97–104, 2004. doi: 10.1016/j.physletb.2004.05.029.

[59] V. Barone, Zhun Lu, and Bo-Qiang Ma. The cos2ϕ asymmetry of drell–yan and j/ψ production in unpolarized pp scattering. *The European Physical Journal C*, 49(4):967–971, Mar 2007. ISSN 1434-6052. doi: 10.1140/epjc/s10052-006-0174-6. URL https://doi.org/10.1140/epjc/s10052-006-0174-6.

[60] A. Sissakian, O. Shevchenko, A. Nagaytsev, and O. Ivanov. Transversity and T-odd PDFs from Drell-Yan processes with p p, p D and D D collisions. *Eur. Phys. J.*, C59:659–673, 2009. doi: 10.1140/epjc/s10052-008-0806-0.

[61] M. Anselmino, V. Barone, and M. Boglione. The Sivers asymmetry in DrellYan production at the J/Ψ peak at COMPASS. *Phys. Lett.*, B770:302–306, 2017. doi: 10.1016/j.physletb.2017.04.074.